Selective PD Measurements on DC Cable Joints Using an HFCT-Balanced Circuit Arrangement

Bernhard Schober, Uwe Schichler
Institute of High Voltage Engineering and System Performance, Graz University of Technology
Graz, Austria
bernhard.schober@tugraz.at

Abstract

Due to the many advantages of medium-voltage (MV) and high-voltage (HV) DC cable transmission lines and the possibility of converting AC transmission to DC transmission, this technology is becoming increasingly relevant. One of the most important diagnosis tools used to investigate the condition of the insulation of high-voltage cables is to apply partial discharge (PD) measurements. Cable joints and terminations are of particular importance, as these represent weak spots due to human interaction. Especially under DC voltage, it is of crucial importance to determine whether the detected PD pulses occur inside or outside the cable accessories.

For this purpose, a PD test method for cable joints using two high-frequency current transformers (HFCT) was optimised with modern electronic devices, including an instrumentation amplifier and a modern PD measuring instrument. Two HFCT with opposite winding directions were placed on the outer semi-conductive layer on both sides of a cable joint. The signals were fed into an instrumentation amplifier to separate the PD pulses originating from inside and outside the cable joint. This method automatically suppresses PD pulses occurring outside the cable joint and was tested on a 12/20 kV AC cable joint under DC voltage with thermal and electrical stress.

1. Introduction

The challenges posed by the energy transition to achieve a sustainable energy supply can only be met by improving the efficiency and increasing the transmission capacity of the high-voltage (HV) transmission and distribution grids. A key technology to meet these challenges is the transmission of electrical energy with DC voltage and HV cables or overhead lines. In general, the public acceptance of cables is greater than that of overhead transmission lines. Medium-voltage (MV) cables also offer the possibility to distribute electrical energy in urban areas.

Since only a limited length of high-voltage cables can be transported via cable drums onshore, cable joints are needed to connect two cables and increase the length of the transmission line. Particularly in the case of MVDC and HVDC technology, the transmission lengths can be increased compared to conventional HVAC lines. Therefore, a larger number of cable joints need to be assembled. Due to human interaction and the assembly of cable joints on-site, these represent weak spots in the transmission system. Selectively determining whether a partial discharge (PD) pulse has occurred inside or outside the DC cable accessories is crucial to increase the reliability of cable systems. Inductively coupled sensors such as high-frequency current transformers (HFCT) offer a simple solution for measuring PD in HV cables. A selective PD measurement can be carried out by using two HFCT and a balanced circuit arrangement similar to that presented in IEC 60270 [1].

2. HFCT-balanced circuit arrangement

2.1. Measurement principle

The HFCT-balanced circuit arrangement uses inductive couplers by means of HFCT and consists of two HFCT per cable joint and a modern electronic device, including an instrumentation amplifier. The basic measurement principle has already been introduced and described in a previous contribution [2]. A PD pulse occurring in the cable or the cable joint produces a travelling wave in both directions in the cable. The propagating electromagnetic waves cause a magnetic flux inside the ferrite core (width b, outer radius r_o, inner radius r_i) of an HFCT and thereby induce a voltage u_i in the windings. By using a measuring resistor R_m, a voltage u_m proportional to the current i_L is produced (Fig. 1).

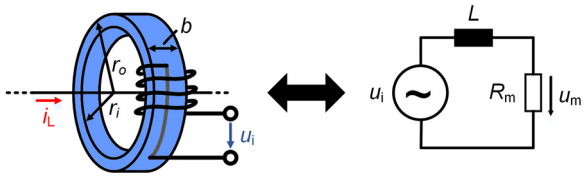

Fig. 1 - Equivalent circuit of an HFCT

The transfer function $Z_T = u_m/i_L$ is described by Eq. (1) and depends on the measuring resistor R_m, the number of windings n and the self-inductance L of the HFCT. This function describes a first-order high-pass filter with a lower cut-off frequency f_{c1}, which is described by Eq. (2).

$$Z_T = \frac{u_m}{i_L} = \frac{R_m}{n} \frac{1}{1 + \frac{R_m}{j\omega L}} \quad (1)$$

$$f_{c1} = \frac{R_m}{2\pi L} \quad (2)$$

The HFCT are placed on the left and right sides of the cable joint on the outer semi-conductive layer of the HV

cable with the cable screen passed around the HFCT. Otherwise, the reciprocating waves in the inner conductor and screen would cancel out the magnetic flux in the ferrite cores.

A travelling wave, regardless of where it originated, induces the voltages u_{HFCT1} and u_{HFCT2} in the HFCT (Fig. 2). By using two identical HFCT with opposite winding directions (HFCT1 and HFTC2) and an instrumentation amplifier (subtractor) with an output voltage $u_{\Delta HFCT} = u_{HFCT1} - u_{HFCT2}$, the PD pulses from outside the cable joint cancel each other out ($u_{\Delta HFCT} = 0$ V), and the PD pulses from inside the cable joint add up (Fig. 3). This selective PD measuring technique automatically suppresses PD pulses occurring outside the cable joint. It is also possible to use a differential amplifier, but an instrumentation amplifier was chosen because of its more effective common-mode rejection ratio. The differential signal $u_{\Delta HFCT}$ can be fed into a PD measuring instrument.

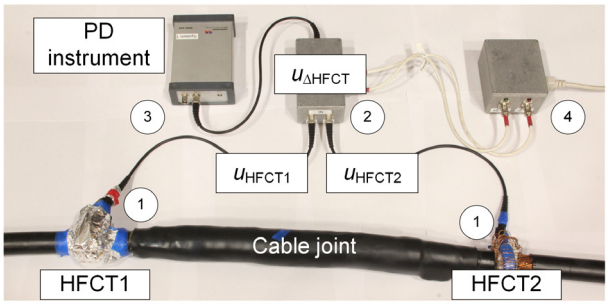

Fig. 2 – HFCT-balanced circuit arrangement for a DC cable joint (1 HFCT, 2 Subtractor, 3 PD instrument, 4 Power supply)

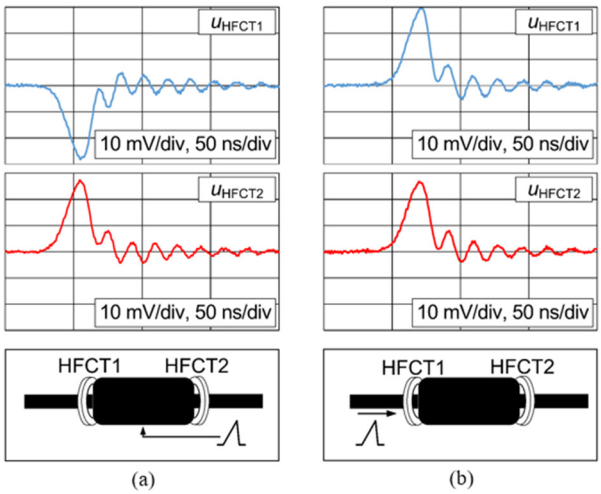

Fig. 3 - Measured voltages at both HFCT as result of a PD pulse occurring a) inside and b) outside the DC cable joint

2.2. Balancing and calibration of the HFCT

When a balanced circuit arrangement such as that described in IEC 60270 is used, the proposed circuit must be calibrated and balanced to attain similar signal paths and thus to suppress the signals occurring outside the cable joint effectively.

The circuit is adjusted with a PD calibrator by injecting and simulating PD pulses from outside the cable joint, as depicted in Fig. 4a. The measuring resistors R_m of the two HFCT and, therefore, their weighting factors a and b are slightly adjusted until the output signal of the instrumentation amplifier $u_{\Delta HFCT}$ reaches a minimum (Eq. (3)). It should be noted that the lower cut-off frequency f_{c1} of the HFCT also changes slightly (Eq. (2)).

$$u_{\Delta HFCT} = a \cdot u_{HFTC1} - b \cdot u_{HFTC2} \qquad (3)$$

After adjusting both signal paths, the circuit is calibrated by injecting PD pulses occurring inside the cable joint, as shown in Fig. 4b.

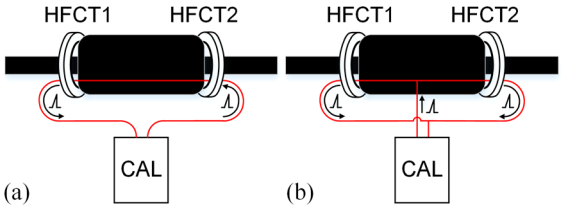

Fig. 4 - a) Balancing and b) calibration of the circuit by simulating PD pulses occurring a) inside and b) outside the cable joint

2.3. Benefits of the HFCT-balanced circuit arrangement

The advantages of the HFCT-balanced circuit arrangement can be summarised as follows:

- Compared to other methods [3], the described HFCT-balanced circuit arrangement requires only one PD measuring instrument and, respectively, one PD channel due to the use of an instrumentation amplifier.
- The technical effort is kept small by mounting both HFCT to a cable joint during installation. This way, low-cost and effective on-site and online PD monitoring with automatic noise suppression is possible.
- It is not necessary to perform additional post-processing of the measured PD pulses to suppress noise and PD pulses from outside the investigated cable joint.

3. Practical design and frequency response

3.1. HFCT

The soft ferrite material Siferrit N30 based on the material MnZn was chosen for the cores of the HFCT. Siferrit N30 has an initial permeability μ_i of 4300 with a variance of ± 25%. The Curie temperature T_C is above 130 °C. The dimensions of the ferrite cores were chosen to be $r_o = 30$ mm, $r_i = 19.5$ mm and $b = 18.8$ mm. The number of windings was defined as $n = 4$ to achieve a high transfer impedance Z_T and a lower cut-off frequency $f_{c1} < 100$ kHz (Eq. (1) and Eq. (2)). The lower and upper cut-off frequencies (-6 dB according to IEC 60270 [1]) were determined with a function generator and an oscilloscope with a measuring resistor $R_m = 50\ \Omega$. Due to the huge variance in the initial permeability μ_i of ± 25% and thus the self-inductance L of the HFCT, the measuring resistor R_m was designed with a potentiometer to accurately balance the circuit, as described previously. The frequency response of the transfer impedance Z_T for $R_m = 50\ \Omega$ is depicted in Fig. 5.

In order to ensure that the measured signals and the frequency responses of both HFCT are as similar as possible and thus to balance and adjust the circuit effectively, the ferrite cores were preselected. Only matching ferrite cores were used for the subsequent investigations and measurements. The properties and characteristics of the designed HFCT are as follows:

- Dimensions in mm: 30 x 19.5 x 18.8 (r_o x r_i x b)
- Number of windings: $n = 4$
- Self-inductance: $L \approx 0.09$ mH
- Measuring resistor range: $R_m = 42\ \Omega$–$68\ \Omega$
- Lower cut-off frequency: $f_{c1} = 70$ kHz ($R_m = 50\ \Omega$)
- Upper cut-off frequency: $f_{c2} > 30$ MHz ($R_m = 50\ \Omega$)
- Transfer impedance: $Z_T = 10.6$ mV/mA ($R_m = 50\ \Omega$)

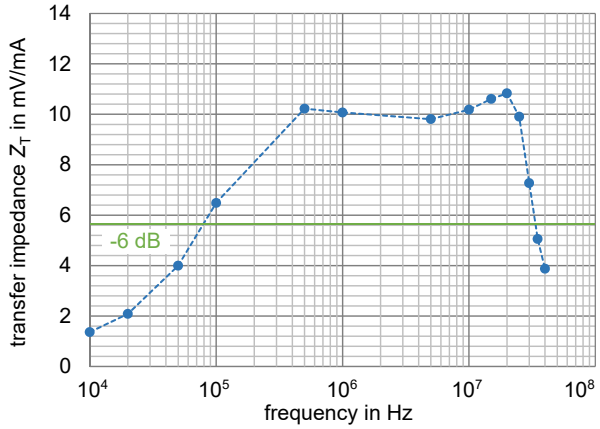

Fig. 5 - Frequency response of the transfer impedance Z_T of the designed HFCT with $R_m = 50\ \Omega$

3.2. Instrumentation amplifier

The balanced circuit arrangement was created with a commercially available instrumentation amplifier. For this purpose, the evaluation board "EVAL-CN0273-EB1Z" from Analog Devices with two ADA4817-2 and one ADA4830-1 was used (Fig. 6) [4]. The circuit offers an input bandwidth of up to 35 MHz, a gain of 5 (and, respectively, 2.5 due to a resistive divider at the output) and a high AC common-mode rejection. To reduce disturbances, the evaluation board as well as the ± 5 V power supply were placed inside a shielded aluminium case.

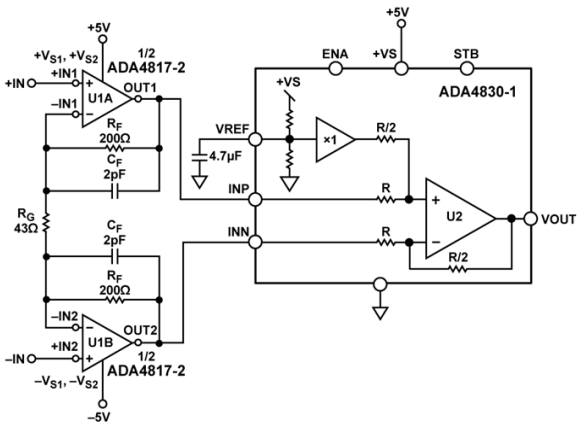

Fig. 6 - Schematic of the investigated instrumentation amplifier evaluation board "EVAL-CN0273-EB1Z" [4]

4. Measurement setup using a 12/20 kV AC cable joint

4.1. PD test circuit and cable joint

The PD measurements were performed on a 12/20 kV AC XLPE cable (NA2XS(F)2Y 1x150/25 RM) and a 12/20 kV AC cable joint. The cable was segmented in 5-m and 10-m parts to the left and right sides of the cable joint (Fig. 7). In the laboratory test setup, the HFCT were placed on the outer semi-conductive layer of the MV cable. The cable screen was passed around the HFCT and shielded with aluminium foil. In a real installation, both HFCT are placed under the screen in the heat shrink tubing of the cable joint. The signal paths of the HFCT could be interrupted remotely by radio frequency (RF) coaxial relays (type CX-230). In this way, the sensitive measuring instruments – the instrumentation amplifier and a PD measuring instrument Omicron MPD 600 (unit 1) – could be protected against overvoltages caused by saturation of the ferrite cores. In parallel, a conventional PD test circuit as described in IEC 60270 with a coupling capacitor of $C_k = 1.2$ nF and a second Omicron MPD 600 device (unit 2) was used to verify the results of the HFCT-balanced circuit arrangement. The DC test voltage of $U_{DC} = \pm 55$ kV was applied to the MV cable by a DC source. To avoid flashovers at the ends of the cable, the sheath, screen and outer semi-conductive layer were removed at about 1 m. Both ends of the cable were connected to induce an AC heating current ($f = 50$ Hz) of about $I = 500$ A in the loop, which meant a temperature in the inner conductor of $\vartheta_{conductor} = 70$ °C.

Omicron PD measuring instruments with a bandwidth of $\Delta f = 800$ kHz and a centre frequency of $f_C = 500$ kHz were chosen to detect the PD pulses. The gain level was set at an appropriate setting to avoid disturbances caused by changing the gain level during the tests. Due to the chosen gain setting and the relatively high noise level caused by the instrumentation amplifier itself, the noise level of unit 1 was about $q_{noise} = 5$ pC. The noise level of unit 2 was lower with $q_{noise} = 2$ pC.

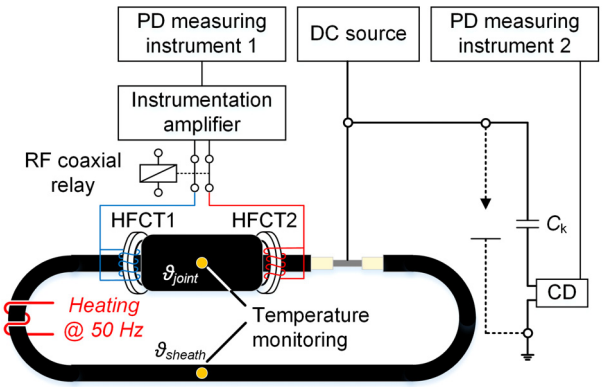

Fig. 7 - PD test circuit with the MV cable joint and the HFCT-balanced circuit arrangement (CD: coupling device)

4.2. Balancing and calibration of the circuit

The HFCT-balanced circuit arrangement was balanced by injecting PD pulses with a PD calibrator at the end of

the cable in parallel to the coupling capacitor C_k. For this purpose, PD pulses with q = 1 nC were injected, and the circuit was adjusted by changing the measuring resistors R_m, as described in section 2.2. After the adjustment, the HFCT-balanced circuit arrangement was calibrated with a PD pulse with q = 100 pC (Fig. 4b). The prior balancing of the circuit was verified by simulating PD pulses occurring outside the cable joint (Fig. 4a). The PD measurement with the coupling capacitor was calibrated with reference to IEC 60270.

4.3. Preliminary testing of the HFCT-balanced circuit arrangement with corona discharges

To verify that the HFCT-balanced circuit arrangement functioned correctly, a needle-plate arrangement was placed in parallel to the coupling capacitor C_k to generate corona discharges and thus PD pulses from outside the cable joint (Fig. 7).

The designed circuit was tested with fixed measuring resistors R_m = 50 Ω and in a balanced mode with adjusted resistors. In addition, only one HFCT was connected to the instrumentation amplifier to investigate the changes by using just one channel. The results were compared with the PD measurement of the coupling capacitor C_k.

Fig. 8 shows a comparison of the average PD magnitudes measured with the different setups at different DC voltages. When using equal signal paths with R_m = 50 Ω for both HFCT (purple and grey bars), a significant reduction in the PD magnitudes of the instrumentation amplifier compared to the PD magnitudes of the coupling capacitor could already be observed ($q_{Ck}/q_{\Delta HFCT} \approx 21$). When using only one HFCT (orange and green bar), the measured PD magnitudes of the instrumentation amplifier increased ($q_{Ck}/q_{\Delta HFCT} \approx 6$). The best results (blue and red bars) were achieved with a balanced circuit ($q_{Ck}/q_{\Delta HFCT} \approx 250$). The results indicate that the HFCT-balanced circuit arrangement can be used to suppress PD pulses from outside the cable joint up to a certain limit. In this example, PD pulses with $q \leq 800$ pC were successfully suppressed by the proposed circuit. Above this level, PD pulses were also measured at the instrumentation amplifier to a certain degree due to the limits in adjusting the analogue circuit.

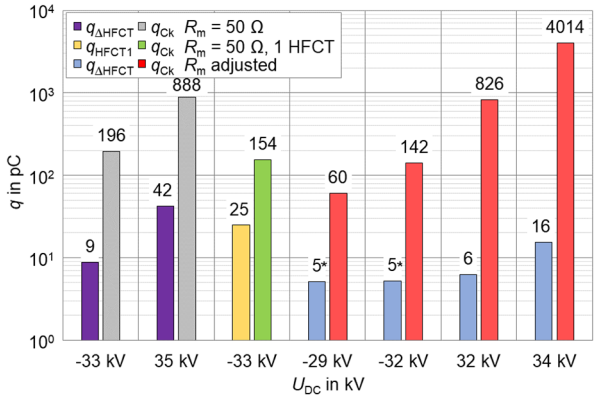

Fig. 8 - Comparison of the average PD magnitudes of corona discharges measured by the HFCT-balanced circuit arrangement with different measuring resistors R_m and the coupling capacitor C_k (*noise level)

4.4. DC test procedures

Four test procedures with different load cycles (LC) and polarity reversals (PR) were defined for electrical and thermal stress at the cable joint and to initialise PD inside the joint. Test cycle 1 was chosen to thermally stress the cable joint under a constant DC voltage with both polarities. Test cycle 2 also included polarity reversals to electrically stress the cable joint. The test cycles 3 and 4 were chosen for the same purpose, but with adjusted durations according to the proposed LC in [5, 6]. The first number in the test cycles describes the duration of the LC, and the second one describes the duration at zero load (ZL):

- Test cycle 1: 2 h/15 min LC with U_{DC} = ± 55 kV
- Test cycle 2: 2 h/15 min LC + PR at U_{DC} = ± 55 kV
- Test cycle 3: 6 h/6 h LC with U_{DC} = ± 55 kV
- Test cycle 4: 6 h/6 h LC + PR at U_{DC} = ± 55 kV

Fig. 9 and Fig. 10 show test cycles 2 and 3, respectively. Each cycle was repeated at least 10 times. The temperatures ϑ of the inner conductor, the cable sheath and the joint were monitored during all test procedures. The temperature of the inner conductor was determined using a reference cable with the same heating current. In total, the cable joint was placed under stress for about 600 h.

Due to the saturation of the ferrite cores, the PD measurements could only be carried out when no AC heating current was applied, since not only PD pulses but also an AC current induces a voltage u_i in the HFCT. To protect the sensitive PD measuring instrument, the RF coaxial relays were synchronised with the AC heating transformers.

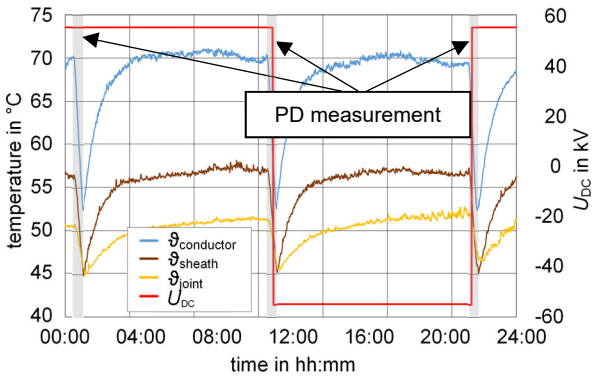

Fig. 9 - Test cycle 2: 2 h/15 min LC + PR at U_{DC} = ± 55 kV

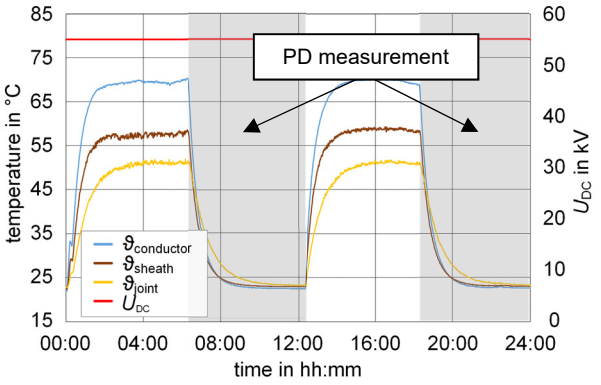

Fig. 10 - Test cycle 3: 6 h/6 h LC with U_{DC} = 55 kV

4.5. Reference measurements at AC voltage

Prior to carrying out the DC test procedures, a PD measurement was performed under AC voltage to detect possible PD defects caused by the installation of the cable and cable joint. The PD measurement was considered as passed if no PD greater than q = 10 pC (according to CENELEC HD-629-1-S3 [7]) occurred within t = 5 min. The AC voltage was chosen with 2.5U_0 = 30 kV higher than suggested in [7]. In addition, this test procedure was repeated after the DC tests to investigate any changes in PD behaviour. The cable and the cable joint passed both tests without any significant PD being observed (Fig. 11).

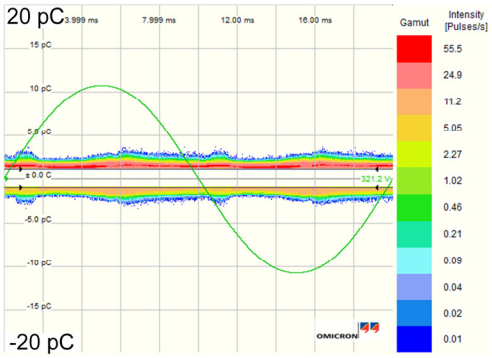

Fig. 11 - PRPD pattern of the PD measurement at U_{AC} = 30 kV for t = 5 min after the DC tests

4.6. Results

In total, the 12/20 kV AC cable joint was placed under thermal and electrical stress under DC voltage with U_{DC} = ± 55 kV for about 600 h. Four different test cycles were defined, with each test cycle being repeated at least 10 times, and PD measurements being performed at ZL. The pulse sequences and NoDi* patterns (as described in [8]) of the detected PD pulses were investigated. The measured PD pulses from the HFCT-balanced circuit arrangement were correlated with those detected at the coupling capacitor C_k, and the place of origin (inside or outside the cable joint) was investigated. PD pulses that could not be correlated with the coupling capacitor were analysed separately. The number of detected potential PD pulses that could have originated inside the cable joint was very low for each performed PD measurement. The PD repetition rate was intermittent and varied between no PD pulses and 30 to 40 PD pulses per PD measurement. Therefore, a classification with NoDi* pattern according to [8] is not sufficient, as at least 1000 PD are needed to obtain significant results. Another possibility is that the measured PD pulses detected at the HFCT-balanced circuit arrangement did not occur inside the cable joint but were large PD from the outside, since the suppression of external PD is just possible to a certain extent, as already described. In addition, due to the open, interference-sensitive test set-up and the short cable lengths, the detected PD pulses may have been external disturbances. In summary, 160 PD pulses were detected that could have originated inside the cable joint with 20 PD pulses with q > 30 pC and 140 PD pulses with $q \leq 30$ pC. Due to the low number of detected PD pulses, no NoDi* pattern was found that indicates the presence of a typical PD defect originating inside the cable joint. Although the place of origin of the PD could not be completely clarified, it can be assumed that the detected PD magnitudes and numbers of PD cannot harm the cable joint.

In real applications with long cable lengths and a closed interference-free test setup, it is easier to separate PD pulses occurring inside the cable joint and external PD pulses and disturbances. In conclusion, the measurement principle of the HFCT-balanced circuit arrangement is suitable for practical use and allows the selective detection of PD pulses in a cable joint to a certain limit. This can be further extended with some improvements, as described in section 5. The measurement principle can also be used for on-site PD measurements of cable joints. Especially in real DC applications, saturation of the ferrite cores is not a problem due to the use of a DC current.

5. Drawbacks and improvements

5.1. High-current HFCT

The saturation of the ferrite cores at high currents (section 4.4) is not a problem in real DC applications, as no voltage u_i is induced in the HFCT by a DC current. For AC applications, it is preferable to use base materials with a higher saturation current for the HFCT cores. Another way to increase the saturation current of the HFCT is to insert air gaps in the ferrite cores.

5.2. Summing amplifier and low-noise circuit

The investigations have shown that the evaluation board "EVAL-CN0273-EB1Z" has a relatively high noise level. To reduce the noise level of the analogue circuit, another board with a summing amplifier was designed and tested. To achieve the same behaviour and to apply the same measurement principle, the winding direction of one HFCT had to be changed (Fig. 3). The schematic of the improved low-noise circuit is shown in Fig. 12.

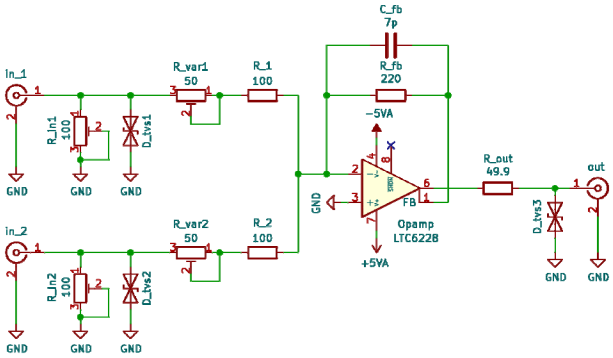

Fig. 12 - Designed circuit of the low-noise summing amplifier

The summing amplifier was built with the low-distortion and low-noise amplifier LTC6228, which has a voltage noise of 0.88 nV/√Hz. The measuring resistors of the HFCT (R_in1 and R_in2), designed as potentiometers, were included directly on the PCB in order to adjust the different frequency behaviours of the two HFCT. The weighting factors of the summing amplifier itself are set

and adjusted with the input resistors R_var1 and R_var2. Therefore, the measuring resistors and the weighting factors can be adjusted separately. The power supply was designed with the low-noise linear regulators LT3045 and LT3094. The entire circuit can be powered by a power bank to achieve galvanic isolation.

A comparison of the balancing of the instrumentation and summing amplifier, as described in section 4.2, showed that the improved circuit has a common-mode rejection ratio that is about 10 times better. For this purpose, both circuits were calibrated with PD pulses with q = 100 pC (Fig. 4b). PD pulses with q = 1 nC, injected at the end of the HV cable by a PD calibrator, were suppressed much more effectively with the modified circuit compared to the instrumentation amplifier due to the improved balancing and adjustment options (Fig. 13). In addition, the noise levels of both circuits were investigated with a PD measuring instrument with the same settings in order to obtain comparable results. The noise level of the PD measuring instrument itself ($q_{noise} \approx 0.12$ pC) was much lower compared to that of the instrumentation and summing amplifier. Nevertheless, the improved circuit has a four-time lower noise level and allows much more sensitive PD measurements to be made with the HFCT-balanced circuit arrangement (Fig. 13).

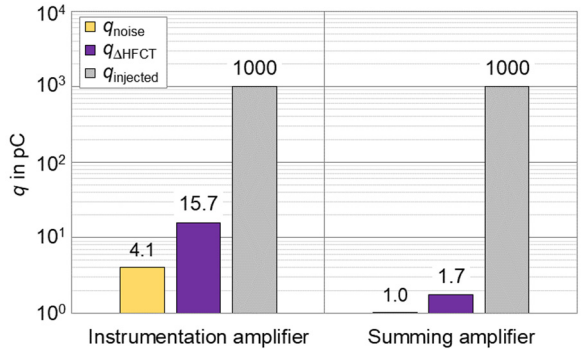

Fig. 13 - Comparison of the noise levels and the common-mode rejection of both circuits by injecting a PD pulse with q = 1 nC at the end of the HV cable

5.3. Balancing of the circuit

As already described, the adjustment of the two HFCT signal paths was only possible to a limited extent with the instrumentation amplifier. This may be due to the huge variance in the initial permeability μ_i of 25% of the used Siferrit N30 cores. Although a prior selection of the cores was made, the HFCT did not show the exact same characteristics. Balancing the circuit by changing the measuring resistors R_m of the HFCT also changed their frequency responses. By using two identical HFCT with the same frequency responses, it is easier to balance the circuit.

6. Summary

The presented HFCT-balanced circuit arrangement applies the measurement principle described in previous research work. It has been improved with modern electronic devices and a modern PD measuring instrument. By using two HFCT per cable joint and an analogue instrumentation amplifier, it was possible to suppress disturbances and PD signals occurring outside the cable joint. The HFCT can be mounted with a small investment of technical effort when installing DC cable joints. This way, effective on-site PD monitoring of DC cable joints can be performed. In addition, several improvements in the HFCT and the analogue circuit are presented.

The circuit was tested on a 12/20 kV AC cable joint with a DC voltage of $U_{DC} = \pm$ 55 kV, and several test procedures were carried out over 600 hours. Four test procedures with different levels of thermal and electrical stress on the cable joint were carried out. Due to the saturation of the ferrite cores at high AC current levels, PD measurements could only be performed at zero load. However, the cable joint withstood the test procedures without a breakdown, and no critical PD pulses were detected during the DC test procedures. Additional PD measurements under AC voltage up to $2.5U_0$ = 30 kV before and after the DC stress were made to confirm these results.

7. References

[1] IEC 60270, “High-voltage test techniques - Partial discharge measurements”, Edition 3.1, 2015.

[2] U. Schichler, “A Sensitive Method for On-Site Partial Discharge Detection on XLPE Cable Joints”, *International Conference on Properties and Applications Materials*, Seoul, Korea, 1997.

[3] F. Esterl and R. Plath, “Sensitive and selective partial discharge measurement method for DC and AC cable joints”, *International Conference on Insulated Power Cables (Jicable'19)*, Versailles, France, 2019.

[4] Analog Devices, “CN0273 – High Speed FET Input Instrumentation Amplifier with Low Input Bias Current and High AC Common-Mode Rejection”, online*: https://www.analog.com/en/design-center/reference-designs/circuits-from-the-lab/cn0273.html#rd-overview*, Accessed 13.03.2022.

[5] A. Buchner and U. Schichler: “Review of CIGRE TB 496 regarding Prequalification Test on Extruded MVDC Cables”, *Nordic Insulation Symposium on Materials, Components and Diagnostics (NORD-IS)*, Tampere, Finland, 2019.

[6] P. Ratheiser and U. Schichler: “Review of IEC 62895 regarding Electrical Type Tests on extruded MVDC Cable Systems”, *International Symposium on HVDC cable systems (Jicable HVDC'21)*, Liège, Belgium, 2021.

[7] CENELEC HD 629-1-S3: “Test requirements for accessories for use on power cables of rated voltage from 3,6/6(7,2) kV up to 20,8/36(42) kV - Part 1: Accessories for cables with extruded insulation”, 2019.

[8] A. Pirker and U. Schichler, “Partial discharge measurement at DC voltage - Evaluation and characterization by NoDi* pattern”, *IEEE Transactions on Dielectrics and Electrical Insulation*, Vol. 25, Issue 3, pp. 883-891, 2018.